Results in Physics 17 (2020) 103063

Contents lists available at ScienceDirect

Results in Physics

journal homepage: www.elsevier.com/locate/rinp

Detection of voltage pulse width effect on charge accumulation in PSCs using EFISHG measurement

Zubair Ahmad[a,*], D. Taguchi[b], Sanghyun Paek[c], Arti Mishra[a], Jolly Bhadra[a], M. Iwamoto[b], T. Manaka[b], Mohammad Khaja Nazeeruddin[c]

[a] Center for Advanced Materials (CAM), Qatar University, P.O.Box 2713, Doha, Qatar
[b] Department of Electrical and Electronic Engineering, Tokyo Institute of Technology, 2-12-1 O-Ookayama, Meguro-Ku, Tokyo 152-8552, Japan
[c] Laboratory of Photonics and Interfaces, Institute of Chemical Sciences and Engineering, École Polytechnique Fédérale de Lausanne, CH-1015 Lausanne, Switzerland

ARTICLE INFO

Keywords:
Triple cation perovskite
Electric field induced second harmonic generation (EFISHG)
Charge accumulation
Pulse width

ABSTRACT

We report the effect of applied pulse width on charge accumulation in triple cation perovskite solar cells (PSCs) during the Electric Field Induced Second Harmonic Generation (EFISHG) measurements. The PSCs were prepared in the n-i-p structure using the layer-by-layer deposition technique. The triple cation perovskite precursor containing $FAPbI_3$, $MAPbBr_3$, and $CsPbI_3$ was used to make the perovskite layer on the FTO/c-TiO_2/mTiO_2 substrates. Spiro OMeTAD was used as a hole transport material over the perovskite active layer, followed by the deposition of Au electrodes. The average power conversion efficiency (PCE) of the fabricated PSCs was 19.17 ± 0.02%. The electric field in the PSCs was selectively probed by the fundamental laser beam wavelength of 960 nm during the EFISHG measurements. Two different pulse widths (100 μs and 50 ms) of the applied potential were used in this study, with consideration of electrode charging and interface charging of PSCs. It has been observed that the pulse width of the applied electric field has a significant effect on the charge accumulation in the PSCs. Using the transient EFISHG measurements, it has also been found that the charging & discharging processes reversibly happen. However, the charging & discharging processes are influenced by remained charges at the interface in PSCs in the investigated triple cations PSCs. The EFISHG results can be well explained by using the Maxwell–Wagner model.

Introduction

A significant factor among the most vital variables that straightforwardly affect the standard of human life is “energy”. To meet the increasing energy requirement in the future, it is essential to seek alternative energy sources. At present, the contribution of renewable energy resources is increasing; however, the low efficiency and high fabrication cost hamper to broaden the application of renewable energy technologies. The emerging trend of green renewable energy has motivated the researchers to develop new photovoltaic materials that could lead to an environmentally friendly as well as economically efficient technology. The versatility of perovskite materials, which can operate as excitonic absorbers for light harvesting as well as promoting efficient charge and energy transport, has triggered the tremendous advancement of perovskite-based solar cell technology [1]. However, PSCs suffer from poor stability when exposed to an ambient environment [2].

It is well recognized that charge carrier processes, including dissociation of excitons into the hole and electron pairs and carriers' lifetime, play a dominant role in producing higher efficiency PSCs [3]. However, complete physics insight is still lacking in terms of interface charge carriers' behavior [4]. The n-i-p PSCs structure simplifies the energy level diagram as well as the carrier path and allows us to know the PSCs in terms of interface charge accumulation due to the Maxwell–Wagner (MW) effect, i.e., due to the relaxation time difference between adjacent two materilas. It is worth mentioning that in addition to the MW type interfacial charge accumulation, the electrode charging, which produces the external electric field and can contribute significantly to the performance of PSCs, due to the dielectric nature of semiconductor halide perovskite materials. Therefore, it is required to distinguish the charge carrier motion as well as the electric field in PSCs for a more in-depth understanding of the complete picture of the charge carriers in PSCs.

The EFISHG technique has been well accounted for to find the charging and discharging processes and electric field distribution accumulating at the layer interfaces of the solar cells [5]. EFISHG

* Corresponding author.
E-mail address: zubairtarar@qu.edu.qa (Z. Ahmad).

https://doi.org/10.1016/j.rinp.2020.103063
Received 30 December 2019; Received in revised form 10 March 2020; Accepted 14 March 2020
Available online 16 March 2020

technique is capable of probing the effect of Maxwell–Wagner type interfaces of the solar cells under short circuit conditions [6]. Our previous studies [7–9] have inspired us to use the EFISHG technique to investigate further the underlying charging process in the PSCs, including the interface charging and electrode charging. In this article, using the EFISHG, the study on the PSCs has been performed and analyzed the effect of the pulse width and presented the charging and discharging processes in the PSCs. Using EFISHG measurements, we determined the transit times and accumulation of charges at the interfaces of the multilayer PSCs structure by selecting the fundamental laser wavelength. Our findings also revealed that, based on the physics of the semiconductor, the interfacial activities of the PSCs could be well analyzed using the MW model. We use this procedure in multi-cation PSCs with usual 3D perovskite layers and lay by layer structures of the 3D and 2D perovskites. A 2D perovskite layer is formed by introducing large-sized organic cation spacers into the perovskite lattice [10], and considered as a potential source of stability enhancement in PSCs [11]. Several methods have been reported to prepare a 2D/3D perovskite heterojunctions [12,13]; however, we used the approach stated by Grancini et al. [14]. This method is capable of producing the 2D/3D heterojunction PSCs, with the power conversion efficiency (PCE) over 20%, by directly depositing a bulk organic cation on a the 3D perovskite surface to induce an in-situ growth of a 2D layer.

Experimental

The n-i-p structured PSCs studied here were prepared strictly following the recipe described in Ref. [15]. Methylammonium bromide (MABr) and formamidinium iodide (FAI) were purchased from Dyesol, while lead iodide (PbI_2) and lead bromide ($PbBr_2$) were obtained from the TCI Chemical Trading Co., Ltd. Cesium iodide (CsI) was bought from TCI Deutschland GmbH. PSCs were fabricated on FTO coated Nippon sheet glass substrates. The substrates were successively cleaned using a detergent solution, acetone, and ethanol in an ultra-sonic cleaner. The compact TiO_2 (c-TiO_2) layer was deposited by spray pyrolysis technique and baked at 450 °C. The precursor solution for the c-TiO_2 layer was prepared by diluting 0.6 ml of titanium diisopropoxide in 9.4 ml ethanol. After cooling the substrates, the mesoporous TiO_2 (m-TiO_2) layer was deposited by a spin coating technique using TiO_2 paste (Dyesol 30 NR-D) diluted in ethanol (1gm/10 ml) followed by sintering at 500 °C for 30 min. The $(FAPbI_3)_{0.85}(MAPbBr_3)_{0.15}$ solution was made by the mixing of PbI_2 (1.15 M), FAI (1.1 M), $PbBr_2$ (0.2 M) and MABr (0.2 M) in a DMF/DMSO (4:1) mixed solvent. An additional solution of $CsPbI_3$ (1.15 M) was also prepared in DMF/DMSO mixed solvent using the same volume ratio of both solvents. To make the triple cation perovskite solution, the $CsPbI_3$ solution was mixed with $(FAPbI_3)_{0.85}(MAPbBr_3)_{0.15}$ solution in a 10:1 volumetric ratio. The perovskite precursor solution was then spin-coated over the c-TiO_2 layer at 4000 rpm for 30 s in a nitrogen environment. Finally, the Spiro-OMeTAD was spin-coated at 4000 rpm for 20 s. 70 mM solution of Spiro-OMeTAD was prepared in chlorobenzene. Finally, the fabrication process was completed by depositing the 70 nm thick Au electrodes using a metal thermal evaporator.

The photovoltaic properties of the PSCs were obtained by measuring the current-voltage (I-V) characteristics of the PSCs using the SunLite Solar Simulator (manufactured by Abet Technologies, USA). The EFISHG technique was used to study the charge accumulation in the PSCs samples. EFISHG spectroscopy will help to understand the device physics of the PSCs. EFISHG can probe the electric field that originates from accumulated charges [16]. Using EFISHG measurements, we determine the transit times of holes and electrons and accumulation of charges at the interfaces of the multilayer PSCs structure by selecting the fundamental laser wavelength. Fig. 1 shows the device structure, measurement scheme, and EFISHG measurement setup. The EFISHG measurement system consisting of a Q-switched Nd: YAG laser connected with an optical parametric oscillator (OPO) was used. The pulsed voltage was synchronized with Q-switched laser pulsing at 10 Hz. The p-polarized fundamental laser beam impinged at an angle of 45° on the PSC, as shown in Fig. 1a, while the second harmonic signals were detected using the photomultiplier tube. AC square voltage as applied to the Au/HTM electrode in reference to Au/FTO electrode. The voltage shape was rectangular with a pulse duration of 50 ms and 100 μs.

Results and discussion

Fig. 2 shows the average current-voltage (I-V) characteristics of the fabricated solar cells (5 samples) under one sun illumination. The key photovoltaic parameters of the samples are given in the table in Fig. 2. The samples exhibited power conversion efficiency (PCE) of 19.17 ± 0.02%. The V_{OC}, J_{SC} and fill factor (FF) are found to be 1.07 ± 0.01 V, 23.6 ± 0.9 mA/cm^2 and 75.9 ± 1%, respectively. During the I-V measurement, the Au electrode was connected to the +ve bias, while the FTO side was grounded.

To examine the effect of the applied voltage pulse and to understand the physics lying behind the charge carrier behavior in the PSCs, the EFISHG spectroscopy was performed. The first step of the EFISHG was the choice of an appropriate fundamental laser beam. For this purpose, we measured the Second Harmonic Generation (SHG) spectrum of the PSC samples under several applied biasing and the fundamental laser wavelength 960 nm was selected to probe the electric fields in samples (see Figure S1, supplementary data). It has been found that the voltage-dependent SHG is stimulated in the PSC samples at SHG wavelength of 480 nm. That is, the generation of SH at 480 nm is confirmed due to the electric field induced second harmonic generation process. In our previous study [17], the EFISHG was first time used to investigate the instability in the PSCs; however, a further analysis was required to clarify the reasons of performance decay in the samples using this technique. Fig. 3 demonstrates the time-resolved EFISHG measurements of the PSCs at a different voltage pulse width of the applied AC square wave signal. Under the AC square voltage application, electrode charge ± Q_e is induced on Au electrode and m-TiO_2/FTO/Au electrode. Consequently, the electric field E_0 is formed in the perovskite layer as [18]:

$$E_0 = \frac{Q_e}{\varepsilon}, \tag{1}$$

where ε is the dielectric constant of the perovskite layer. Note that a positive electric field $E_0 > 0$ is defined as that the field is pointing in the direction from the Au electrode to the m-TiO_2 surface. Afterward, the carriers are injected from the electrode surface, and the accumulated charge Q_s at the HTM/perovskite layer additionally form an electric field and total electric field in the perovskite layer change to [19]:

$$E_0' = \frac{Q_e}{\varepsilon} + \frac{1}{d_2}\frac{Q_s}{C_1 + C_2}, \tag{2}$$

where d_2 is perovskite layer thickness, C_1 and C_2 are capacitance of HTM layer and perovskite layer, respectively. In EFISHG measurement, we probe the electric field E_0 (E'_0) as the optical second-harmonic light intensity is promotional to both E_0 ($I_{shg} \propto |E_0|^2$) and E_0' ($I_{shg} \propto |E'_0|^2$), while the E_0 and E'_0 are directly originating from electrode charge (Q_e) and accumulated charge Q_s, respectively. When the applied electric field intensity was switched by changing the applied voltage from 0 to −ve potential, the SHG intensity was found to be proportion to this externally applied voltage. The SHG intensity was found to rise swiftly with a time 10^{-6} s according to the measurement circuit time constant. The electric field is formed in the perovskite layer due to the electrode charge Q_e, and once the carriers are injected into the perovskite layer, these injected carriers Q_s form a space charge electric field and change the total electric field in the layers. In Fig. 3(a), after voltage application of −5 V, SHG increase at 10^{-6} s as well, and after that, the SHG

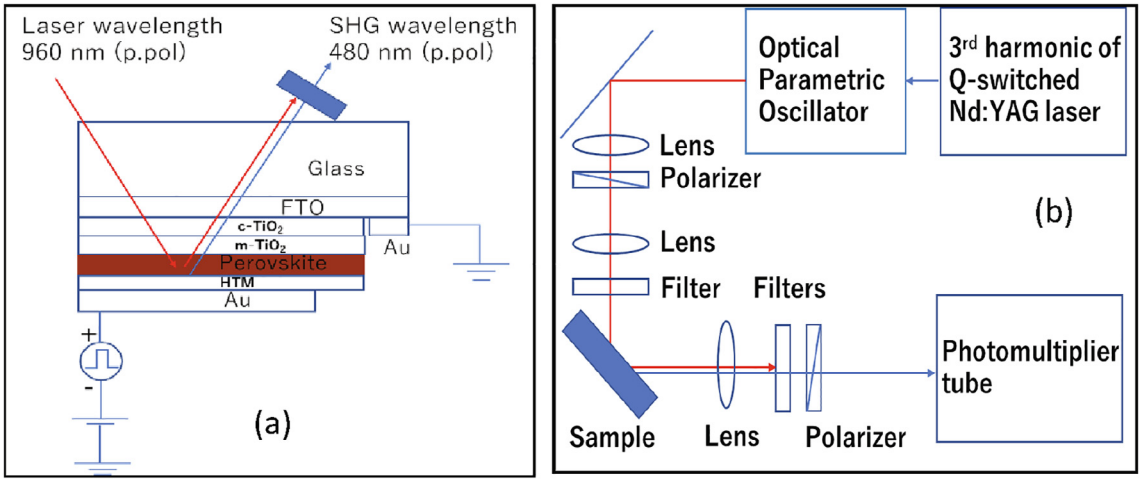

Fig. 1. (a) Schematic of the connections for the EFISHG measurements. (b) Experimental setup for EFISHG measurements.

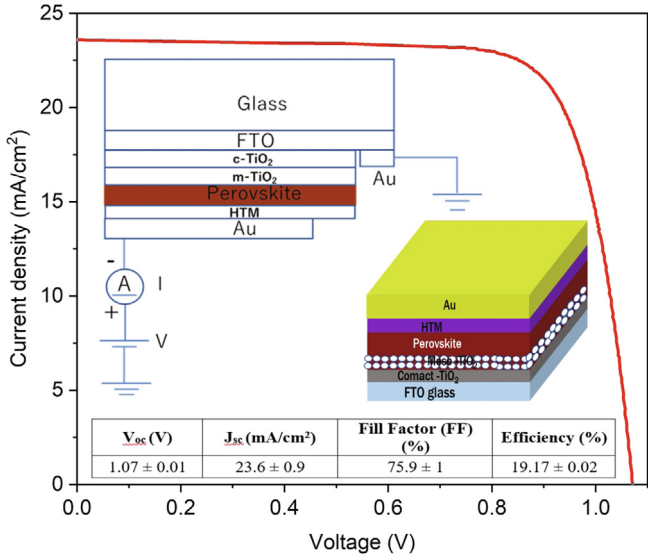

Fig. 2. I-V characteristics of the PSCs. The inset shows the device structure and connection scheme during the I-V measurement. The table in the inset shows the photovoltaic parameters and variation.

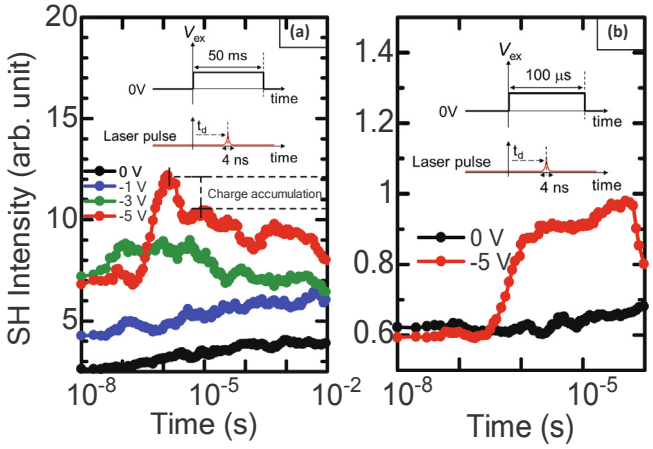

Fig. 3. TR-EFISHG measurements of the PSCs under different applied fields and pulse width. (a) The pulse width is 50 ms. (b) The pulse width is 100 µs.

intensity begins to decrease. To be precise, the findings revealed that the SHG signal in the samples increased until 10^{-6} s because of the electrode charging. Later, SHG intensity decreased due to the charge carrier accumulation followed by the transport of injected carriers. Considering the carrier impeding property of the perovskite layer, we assume that the decrease of the SHG intensity is due to accumulation of the charges in either perovskite layer or at the HTM/perovskite layer. The transient EFISHG specified that the local electric field changed in the perovskite layer over the time range from 10^{-6} to 10^{-2} s, because of the charge injection and their transport. These results are dissimilar to the samples measured when the smaller voltage pulse was applied, where the number of injected carriers is restricted. Fig. 3(b) shows EFISHG results of PSCs using the shorter voltage pulse.

Fig. 4 shows the time-resolved EFISHG measurements of the PSCs with the delay time in the increasing and decreasing order. Even though both the curves are looking similar, however, a close-by glance on the figure indicates that there is charge accumulation that exists when we scanned the sample from the opposite sides. In Fig. 4a, the EFISHG signals changed principally in two steps. First, the EFISHG signal intensity increased because of the electrostatic field developed due to the electrode charging. During this process, the applied external electric field changed with a time response of $E_e(t) = (V_{ex}/d)\ (1 - \exp(-t/t_{RC}))$ (d is the effective thickness of dielectric layer and t_{RC} is the circuit response time and can be represented by $t_{RC} = RC$, Where R is the sheet

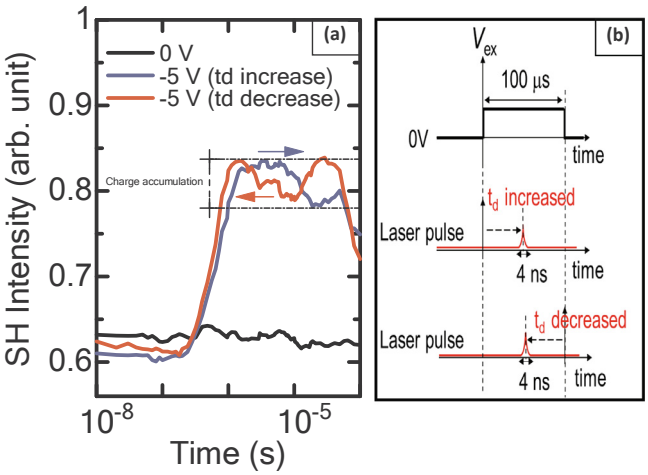

Fig. 4. (a) TR-EFISHG measurements of the PSCs with the increasing and decreasing delay time (t_d). (b) The timing chart of the laser pulse and voltage pulse in TR-EFISHG measurement.

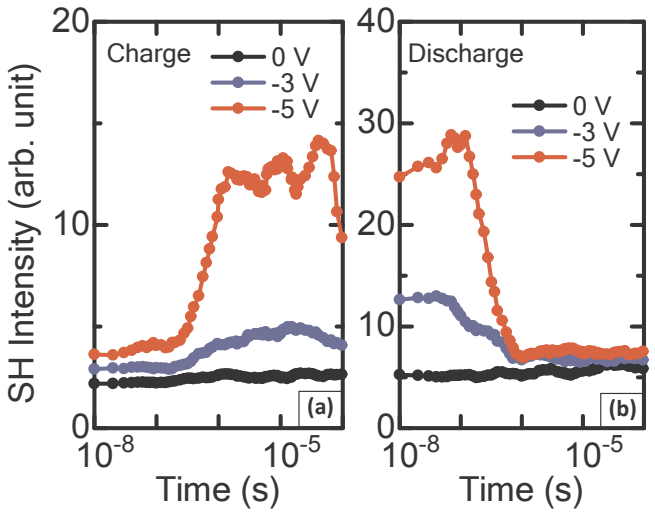

Fig. 5. (a) Charge and (b) discharge graph of the TR-EFISHG measurements with a pulse width 100 μs.

resistance of FTO substrate and *C* is the static capacitance of the PSC. In the 2nd step, the decrease in the EFISHG signal intensity was witnessed under the negative applied voltage with t_d in the increasing order. In this case, the Maxwell-Wagner effect charges are accumulated at interfaces, and a space charge field (E_s) is formed. Hence, the space charge field changed the resultant total electrostatic field in PSCs, leading to a decrease of SH intensity (see Eq. (2)). This step took place with a response time of Maxwell-Wagner charging t_{MW}. However, this effect is not exactly similar when the t_d is in the decreasing order, possibly because the transport is effectively governed by the remained charge at the interfaces.

Fig. 5 shows the charging/discharging curves during the EFISHG measurements of the PSCs under applied AC square wave voltage (0 V to −5V) with a pulse width of 100 μs. The results indicate that the charging and discharging process is reversible. There is no breakdown in the sample, and charge accumulation at 100 μs is not dominant. Charging and discharging times were approximately found to be the same (in the range of 10^{-6} s). Here it is important to note that the interfacial carrier charging process can be mapped out through the local electric field (E_0), where the (E_0) can be determined by the EFISHG signal I_{shg} using the relation $I_{shg} \propto |E_0|^2$.

Conclusion

In conclusion, we found that the EFISHG measurements could effectively characterize the transient carrier behavior in the PSCs. It has been observed that the pulse width of the applied electric field has a significant effect on the charge accumulation in the PSCs, more prolonged the pulse width more the charge accumulation. The charging & discharging processes are found to be reversible. The Maxwell–Wagner model based on dielectric physics can explain these results.

Declaration of Competing Interest

The authors declare that they have no known competing financial interests or personal relationships that could have appeared to influence the work reported in this paper.

Acknowledgments

This publication was made possible by the NPRP award [NPRP11S-1210-170080] from Qatar National Research Fund (a member of the Qatar Foundation). The findings made herein are solely the responsibility of the authors.

Appendix A. Supplementary data

Supplementary data to this article can be found online at https://doi.org/10.1016/j.rinp.2020.103063.

References

[1] Chen Y, et al. 30% enhancement of efficiency in layered 2D perovskites absorbers by employing homo-tandem structures. Solar RRL 2019;3(6):1900083.
[2] Zhao X, Park N-G. Stability issues on perovskite solar cells. in Photonics. Multidisciplinary Digital Publishing Institute; 2015.
[3] Głowienka D, Szmytkowski J. Numerical modeling of exciton impact in two crystalographic phases of the organo-lead halide perovskite (CH3NH3PbI3) solar cell. Semicond Sci Technol 2019;34(3):035018.
[4] Lu C, et al. Carrier transfer behaviors at perovskite/contact layer heterojunctions in perovskite solar cells. Adv Mater Interfaces 2019;6(2). 1801253.
[5] Chen X, et al. Analysis of anomalous discharging processes in pentacene/C60 double-layer organic solar cell. Jpn J Appl Phys 2012;51(2S). 02BK01.
[6] Chen X, et al. Analysis of interfacial charging process in pentacene/C60/bathocuproine triple-layer organic solar cells using a maxwell-wagner model. Jpn J Appl Phys 2013;52(4S). 04CR05.
[7] Win LLY, Taguchi D, Manaka T. Transient carrier visualization of organic-inorganic hybrid perovskite thin films by using time-resolved microscopic second-harmonic generation (TRM-SHG). Org Electron 2019;75:105416.
[8] Chen X, et al. Study of multiple photovoltaic processes in stacked organic active layers. Org Electron 2014;15(9).
[9] Chen X, et al. Selective observation of photo-induced electric fields inside different material components in bulk-heterojunction organic solar cell. Appl Phys Lett 2014;104(1):013306.
[10] Yang R, et al. Oriented quasi-2D perovskites for high performance optoelectronic devices. Adv. Mater. 2018;30(51):1804771.
[11] Cho KT, et al. Selective growth of layered perovskites for stable and efficient photovoltaics. Energy Environ. Sci. 2018;11(4):952–9.
[12] Lee K, et al. A highly stable and efficient carbon electrode-based perovskite solar cell achieved via interfacial growth of 2D PEA 2 PbI 4 perovskite. J. Mater. Chem. A 2018;6(47):24560–8.
[13] Niu T, et al. Interfacial engineering at the 2D/3D heterojunction for high-performance perovskite solar cells. Nano Lett. 2019;19(10):7181–90.
[14] Grancini G, et al. One-year stable perovskite solar cells by 2D/3D interface engineering. Nat Commun 2017;8(1):1–8.
[15] Cho KT, et al. Selective growth of layered perovskites for stable and efficient photovoltaics. Energy Environ Sci 2018;11(4):952–9.
[16] Ahmad Z, et al. A way for studying the impact of PEDOT: PSS interface layer on carrier transport in PCDTBT: PC71BM bulk hetero junction solar cells by electric field induced optical second harmonic generation measurement. J Appl Phys 2015;117(16):163101.
[17] Ahmad Z, et al. Stability in 3D and 2D/3D hybrid perovskite solar cells studied by EFISHG and IS techniques under light and heat soaking. Org Electron 2019;66:7–12.
[18] Maxwell JC. A treatise on electricity and magnetism. Clarendon press; 1881.
[19] Manaka T, et al. Diffusionlike electric-field migration in the channel of organic field-effect transistors. Phys Rev B 2008;78(12):121302.